Accepted Manuscript

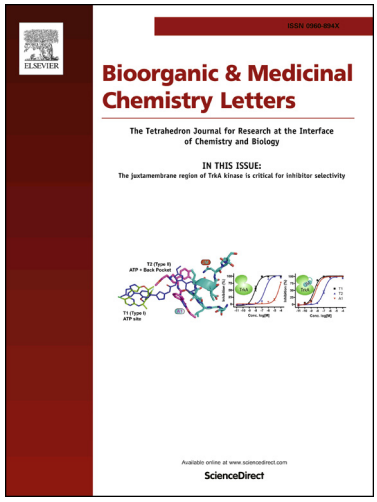

Discovery of a series of 8-(1-phenylpyrrolidin-2-yl)-6-carboxamide-2-morpholino-4H-chromen-4-one as PI3Kβ/δ inhibitors for the treatment of PTEN-deficient tumours

Bernard Barlaam, Sabina Cosulich, Sébastien Degorce, Rebecca Ellston, Martina Fitzek, Stephen Green, Urs Hancox, Christine Lambert-van der Brempt, Jean-Jacques Lohmann, Mickaël Maudet, Rémy Morgentin, Patrick Plé, Lara Ward, Nicolas Warin

PII: S0960-894X(17)30262-7
DOI: http://dx.doi.org/10.1016/j.bmcl.2017.03.027
Reference: BMCL 24779

To appear in: *Bioorganic & Medicinal Chemistry Letters*

Received Date: 13 February 2017
Revised Date: 9 March 2017
Accepted Date: 12 March 2017

Please cite this article as: Barlaam, B., Cosulich, S., Degorce, S., Ellston, R., Fitzek, M., Green, S., Hancox, U., Lambert-van der Brempt, C., Lohmann, J-J., Maudet, M., Morgentin, R., Plé, P., Ward, L., Warin, N., Discovery of a series of 8-(1-phenylpyrrolidin-2-yl)-6-carboxamide-2-morpholino-4H-chromen-4-one as PI3Kβ/δ inhibitors for the treatment of PTEN-deficient tumours, *Bioorganic & Medicinal Chemistry Letters* (2017), doi: http://dx.doi.org/10.1016/j.bmcl.2017.03.027

Bioorganic & Medicinal Chemistry Letters
journal homepage: www.elsevier.com

Discovery of a series of 8-(1-phenylpyrrolidin-2-yl)-6-carboxamide-2-morpholino-4H-chromen-4-one as PI3Kβ/δ inhibitors for the treatment of PTEN-deficient tumours.

Bernard Barlaam,*[,a] Sabina Cosulich,[a] Sébastien Degorce,[a] Rebecca Ellston,[b] Martina Fitzek,[b] Stephen Green,[b] Urs Hancox,[b] Christine Lambert-van der Brempt,[c] Jean-Jacques Lohmann,[c] Mickaël Maudet,[c] Rémy Morgentin,[c] Patrick Plé,[c] Lara Ward,[b] Nicolas Warin[c]

[a] *IMED Oncology, AstraZeneca, Darwin Building, Cambridge Science Park, 319 Milton Road, Cambridge CB4 0WG, United Kingdom.*
[b] *IMED Oncology, AstraZeneca, Alderley Park, Macclesfield, Cheshire SK10 4TG, United Kingdom.*
[c] *AstraZeneca, Centre de Recherches, Z.I. La Pompelle, B.P. 1050, Chemin de Vrilly, 51689 Reims, Cedex 2, France*

ARTICLE INFO

Article history:
Received
Revised
Accepted
Available online

Keywords:
PI3Kβ/δ inhibitor
Rational design
PTEN-deficient tumours

ABSTRACT

Attempts to lock the active conformation of compound **4**, a PI3Kβ/δ inhibitor (PI3Kβ cell IC_{50} 0.015 μM), led to the discovery of a series of 8-(1-phenylpyrrolidin-2-yl)-6-carboxamide-2-morpholino-4H-chromen-4-ones, which showed high levels of potency and selectivity as PI3Kβ/δ inhibitors. Compound **10** proved exquisitely potent and selective: PI3Kβ cell IC_{50} 0.0011 μM in PTEN null MDA-MB-468 cell and PI3Kδ cell IC_{50} 0.014 μM in Jeko-1 B-cell, and exhibited suitable physical properties for oral administration. In vivo, compound **10** showed profound pharmacodynamic modulation of AKT phosphorylation in a mouse PTEN-null PC3 prostate tumour xenograft after a single oral dose and gave excellent tumour growth inhibition in the same model after chronic oral dosing. Based on these results, compound **10** was selected as one of our PI3Kβ/δ preclinical candidates.

The PI3K-AKT signalling pathway plays a critical role in cell growth, proliferation, motility and survival. In human cancer, this pathway is activated by several mechanisms, including somatic mutations, deletions and amplifications. Within this pathway, Class I phosphoinositide 3-kinases (PI3Ks) have emerged as attractive targets for the treatment of cancers. This class is composed of 4 members: PI3Kα, PI3Kβ, PI3Kγ and PI3Kδ. All isoforms phosphorylate phosphatidylinositol (4,5)-bisphosphate (PIP2) to generate phosphatidylinositol (3,4,5)-triphosphate (PIP3). PIP3 acts as a second messenger to trigger a diverse set of signalling cascades, whilst the tumour suppressor PTEN (phosphatase and tensin homolog) reverses this process.[1]

While the different members of Class I PI3Ks were originally thought to be redundant in function, the generation of isoform selective inhibitors has started to elucidate individual distinct functions for these lipid kinases.[2] For instance, PI3Kδ has been shown to play a critical role in B-cell signalling in response to a number of cytokines and chemokines. Specific inhibition of PI3Kδ has been shown to have activity in human B-cell cancers such as chronic lymphocytic leukemia (CLL) and indolent non-Hodgkin lymphoma (iNHL).[3] Similarly, inhibition of PI3Kβ is thought to be important in PTEN-deficient tumours, as deletion of PI3Kβ was shown to markedly impair tumorigenesis driven by the loss of PTEN.[4] These results have prompted drug discovery efforts to find selective orally available PI3Kβ inhibitors and, as a result, many PI3Kβ selective inhibitors have been disclosed in recent years.[5]

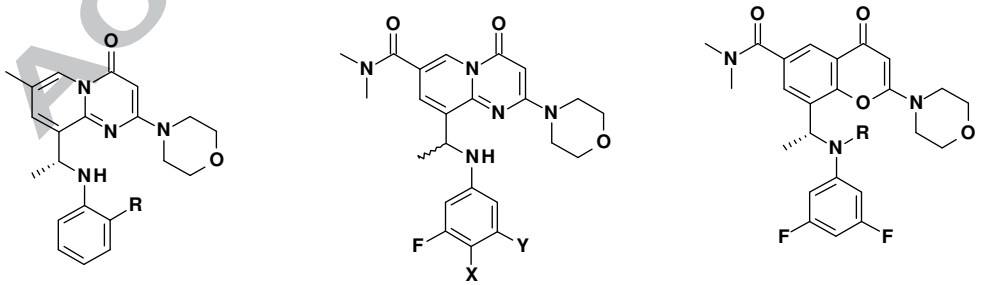

(*R*)-TGX221 (R= H)
AZD6482 (R= CO_2H)

1 (X= H, Y= F), (*R*)-enantiomer
2 (X= F, Y= H), (-)-enantiomer

3 AZD8186, R= H
4 R= Me

Figure 1. Structures of some pyridopyrimidone- and chromenone-based PI3Kβ/δ inhibitors

Initial work at AstraZeneca resulted in the discovery of AZD6482,[6] a PI3Kβ inhibitor showing inhibition of platelet aggregation suitable for short intravenous infusion in humans. We subsequently reported further optimisation of AZD6482 to potent and orally available PI3Kβ/δ inhibitors.[7-9] An essential aspect of this work was the removal of the carboxylic acid, for which we had to compensate the increase of lipophilicity in this pyridopyrimidone series (measured $logD_{7.4}$ of TGX-221: 3.6). Substitution with an amide at the 7-position of the pyridopyrimidone core afforded orally available compounds, as exemplified by **1** and **2**, the latter showing potent tumour growth inhibition in a PTEN-deficient tumour model.[7b] Scaffold hopping to the more hydrophilic chromenone increased human metabolic stability and led to the identification of the clinical candidate **3** (measured $logD_{7.4}$: 2.3), known as AZD8186, currently in phase I clinical trials.[8] Interestingly, during this work, we showed that alkylation of the nitrogen of the aniline by a methyl group (i.e. **4**) was tolerated with minimal loss of potency (PI3Kβ cell IC_{50} 0.015 μM for **4** vs. 0.003 μM for **3**). We previously reported our homology model of PI3Kβ kinase, the T-shaped active conformation for this series of PI3Kβ inhibitors and the key interactions with the PI3Kβ kinase.[7b] On the basis of the docking of **4** in this model, the methyl on the asymmetric carbon bearing the aniline and the methyl on the nitrogen of the aniline would be on the same side and, therefore, might offer the possibility for cyclisation. We hypothesised that cyclisation may limit conformational freedom even further and lock the molecule into its active conformation. Modelling work suggested that a five membered ring would have the required conformation (see overlay in Figure 2). The pyrrolidine linker was predicted to overlay very well with that of the acyclic linker, although the phenyl ring could be slightly shifted. This was thought to potentially change the SAR previously reported around optimal substitution of the aniline.

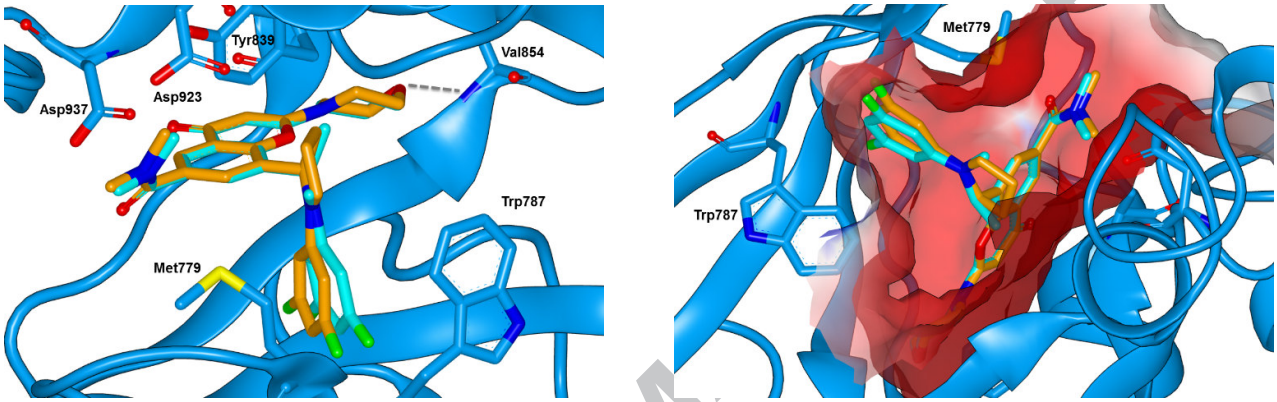

Figure 2: Overlay of the docked structures for **4** (cyan) and **8** (orange) into the previously described homology model of PI3Kβ (a) Ribbon diagram showing the predicted conformation of the pyrolidine linker in relation to the acyclic version. b) Surface (in red) showing the available pocket focused on the 3,5-difluorophenyl moiety.

We describe therein the discovery of a series of 8-(1-phenylpyrrolidin-2-yl)-6-carboxamide-2-morpholino-4H-chromen-4-one as orally available PI3Kβ/δ selective inhibitors and their potential application as anticancer agents in PTEN-deficient tumours. Compounds **5-15** were evaluated as racemates or pure enantiomers as indicated in Table 1, and selectivity among PI3K kinases is reported for selected compounds in Table 2.[10]

Compounds **5-15** were made according to Schemes 1-4. We previously reported the synthesis of dimethyl amide **17**[9] from **16**,[8] via a one-pot saponification / amide coupling with dimethyl amine via the activated 4,6-methoxytriazine-2-oxy ester. We anticipated accessing compound **5** from **19**, which would be obtained from **17** by palladium-catalyzed arylation of N-Boc pyrrolidine with the option of high enantioselectivity (Scheme 1, dotted arrow).[11] However, despite significant optimisation, **19** was obtained only in a very modest yield.[12]

We turned to another strategy (Scheme 1): Suzuki coupling of **17** with *N*-Boc-pyrrole-2-boronic acid proceeded with good yield to give **18**. Selective hydrogenation of the Boc-pyrrole **18** gave pyrrolidine **19**. Boc deprotection followed by Buchwald reaction with the corresponding aryl bromide afforded **5** as a racemate, and **6** as a pure enantiomer after preparative chiral chromatography. A similar sequence was developed from ester **16**, allowing amide variation at the last step (e.g. compounds **8-9** and **13**, Scheme 2).

Separation of the enantiomers at the *N*-Boc pyrrolidine **22** stage was carried out and provided the (*R*)-*N*-Boc-pyrrolidine **25** and (*S*)-*N*-Boc-pyrrolidine **26**. Configuration of each enantiomer was assigned by X-ray structure determination of **29**, the (*S,S*) tartrate salt of **28**, obtained from **26** after Boc deprotection.[13] The Boc deprotection of **25** provided enantiomerically pure **27** having the (*R*) configuration.

A similar sequence as in Scheme 2 was carried out: Buchwald coupling with the appropriate aryl bromide provided esters **30-32** which were converted into the corresponding amides **6-7**, **10-12** and **15** (Scheme 3).

An alternative route was developed in Scheme 4. The one-pot saponification / amide coupling with morpholine via the activated 4,6-methoxytriazine-2-oxy ester gave **33**. Heck coupling with *N*-Boc-2,3-dihydropyrrole afforded the 2,5-dihydropyrrole **34** (contaminated with the 2,3-dihydropyrrole analogue). Boc deprotection with trifluoroacetic acid and hydrogenation afforded pyrrolidine **35**, which was then coupled with 1-bromo-3,5-fluorobenzene or 1-bromo-4-fluorobenzene under Buchwald conditions to give **10** or **14** after chiral chromatography.[13]

Initial compounds **5** and **6** showed exquisitely strong PI3Kβ inhibition (cellular IC_{50} around 0.003 μM, Table 1). This level of potency was unprecedented for unsubstituted or 4-fluoro phenyl in earlier series (e.g. PI3Kβ cellular IC_{50} 0.128 μM for the racemic 4-fluorophenyl analogue of **3**).[7b,8] Selectivity over PI3Kα and PI3Kγ was maintained as illustrated by **6** (PI3Kα cellular IC_{50} 0.18 μM; PI3Kα/β cellular selectivity ratio: 50; PI3Kγ enzyme IC_{50} 0.33 μM), while PI3Kδ activity was conserved (PI3Kδ enzyme IC_{50} 0.0082 μM). We had previously shown that 3-mono- or 3,5-di-substitution of the phenyl with fluorine was preferred in the earlier series: indeed compounds **7** and **8** showed increased PI3Kβ potency (cellular IC_{50} 0.0012 μM for both), but not to the same extent, presumably owing

to slight differences in the way the phenyl ring fits in the active site. High permeability and evidence of oral exposure was seen in this series as exemplified by **5** and **8**, but these early compounds **5-8** showed moderate to high human hepatocyte turnover. We turned our attention to the amide part of the molecule, with the intention to reduce lipophilicity as a way of increasing metabolic stability of our initial molecules. Many amides (i.e. **9-13**) were tolerated and maintained high levels of potency. Gratifyingly, less lipophilic compounds **9** and **13** had improved metabolic stability, but introduction of an additional H-bond donor (hydroxyl) compromised permeability (i.e. Caco-2 P_{app} $2.6x10^{-6}$ cm/s for **9**) and, as a consequence, oral exposure in mouse was low. Similarly, the slightly basic *N*-methyl piperazine **11** had only modest permeability (i.e. Caco-2 P_{app} $3.3x10^{-6}$ cm/s). Overall, the most interesting amide was morpholine **10**, displaying high permeability (i.e. Caco-2 P_{app} 18.10^{-6} cm/s), low human hepatocyte turnover (Cl_{int} 5 µL/min/10^6 cell) and acceptable mouse oral exposure (AUC 2.8 µM.h following a 30 µmol/kg oral dose). Pharmacokinetics of **10** and **15** were evaluated in mouse (see Table 3). The observed in vivo clearance was well predicted from in vitro mouse hepatocytes, suggesting that clearance was essentially metabolic in the liver.

Based on its overall profile and properties, compound **10** was selected for further evaluation. Compound **10** was profiled in dog pharmacokinetics, confirming that in vivo clearance could essentially be predicted from in vitro hepatocytes. Compound **10** (from crystalline material, melting point 180 °C) had excellent aqueous solubility: 430 µg/mL in FASSIF (Fasted Simulated Intestinal Fluid) and 230 µg/mL in aqueous buffer (pH 6.5) and did not show any significant hERG inhibition (hERG IC_{50} 45 µM) or CYP P450 inhibition (IC_{50} >30 µM against CYP 1A2, 2C9, 2C19, 2D6 and 3A4).

The broader kinase selectivity of **10** was evaluated in several kinase panels. **10** showed excellent selectivity in a panel of 71 protein kinases ('Dundee University protein kinase' panel) at 1 µM, showing less than 25% of inhibition against all kinases, except MNK1 and MARK4 respectively 36% and 32% of inhibition. Selectivity among lipid kinases was assessed in a panel of 15 kinases ('Dundee University lipid kinase' panel), where no significant activity (IC_{50} >50 µM for all kinases, except SphK1 IC_{50} 29 µM) was seen outside of PI3K class I enzymes. Bespoke kinase assays confirmed selectivity against selected kinases from the closely related PIKK family (e.g. m-TOR IC_{50} 42 µM). The selectivity profile of **10** among the PI3K isoforms was evaluated in cell based assays: **10** is a potent inhibitor of PI3Kβ [IC_{50} 0.0011 µM (**+/-** SEM: 0.0002)] and PI3Kδ [IC_{50} 0.014 µM (**+/-** SEM: 0.001)], with good selectivity over PI3Kα [IC_{50} 0.14 µM (**+/-** SEM: 0.06)] and PI3Kγ (IC_{50} 1.5 µM)[10]

Compound **10** was selected for in vivo evaluation in PTEN-deficient tumour models. In an acute pharmacodynamic experiment following a single oral dose (100 mg/kg or 30 mg/kg) of **10** in nude mice bearing PTEN-deficient PC3 prostate tumour xenografts, target modulation was assessed by measuring AKT phosphorylation levels at Ser473 at 30 minutes, 2 and 8 hours. At both doses, strong inhibition of AKT phosphorylation was observed at early time points, with still significant inhibition at 8 hours (see Figure 3).

The antitumour activity of **10** was evaluated in the PTEN-deficient PC3 prostate tumour xenograft model in nude mice at 100 mg/kg b.i.d. and 50 mg/kg b.i.d. Strong inhibition of tumour growth was seen at both doses, resp. 83% and 71% tumour growth inhibition at 100 mg/kg and 50 mg/kg b.i.d. at the end of the study (Figure 4).

In summary, based on the docking of **4** in our PI3Kβ homology model and the analysis of its active conformation, we have designed a series of 8-(1-phenylpyrrolidin-2-yl)-6-carboxamide-2-morpholino-4H-chromen-4-one as PI3Kβ/δ inhibitors. Optimisation of this novel series led to compound **10**, a potent PI3Kβ/δ inhibitors with excellent selectivity vs. PI3Kα and PI3Kγ, and suitable physical properties for oral administration. Compound **10** showed profound pharmacodynamic modulation of AKT phosphorylation in PTEN-deficient PC3 prostate tumour bearing mice after oral administration and gave significant inhibition of tumour growth in the same xenograft model. Compound **10** was selected as a PI3Kβ/δ preclinical candidate alongside AZD8186.

Figure 3. Inhibition of AKT phosphorylation in the PC3 xenograft model in nude mice following oral administration of compound **10** (100 mg/kg and 30 mg/kg) and associated free plasma concentration at 30 minutes, 2 hours and 8 hours.

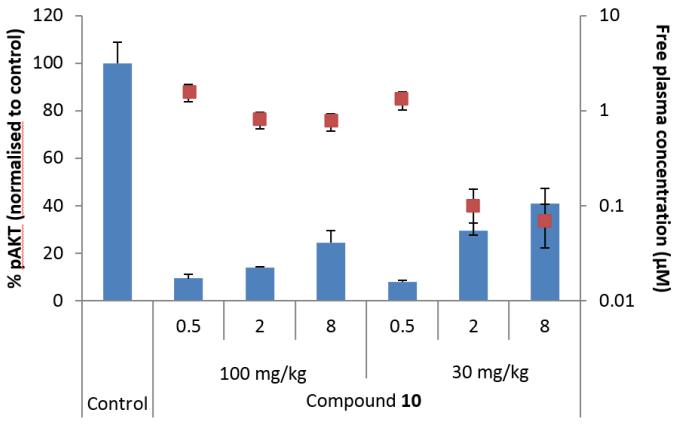

Figure 4. Tumour growth inhibition in the PC3 xenograft model in nude mice following chronic oral administration of compound **10** (100 mg/kg b.i.d. and 50 mg/kg b.i.d.).

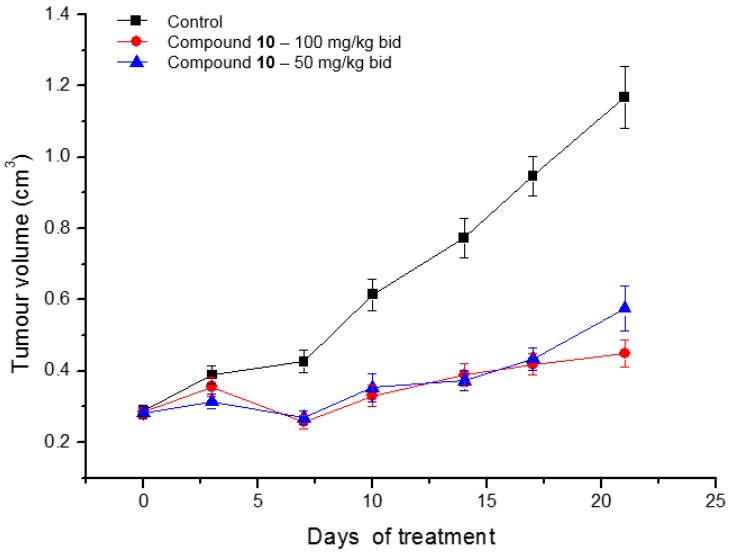

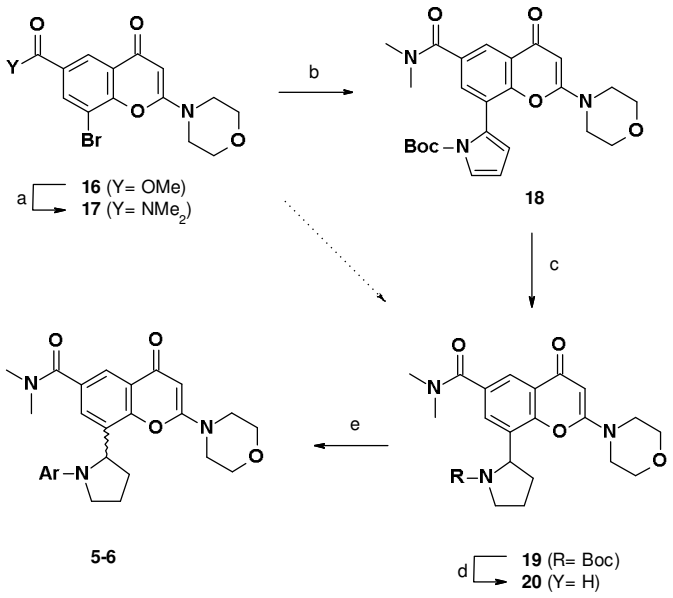

Scheme 1. Synthesis of compounds **5-6**. (a) KOH (2 eq.), H_2O, rt, 4 h; $Me_2NH.HCl$ (3 eq.), 2-Cl-4,6-MeO-1,3,5-triazine (4.3 eq.), *N*-Me-morpholine (7 eq.), H_2O, rt to 70 °C, 78%; (b) *N*-Boc-pyrrole-2-boronic acid (1.2 eq), $(PPh_3)_2PdCl_2$ (0.02 eq.), Na_2CO_3, DME-water, 80 °C, 8 h, 62%; (c) 5% Rh/Al_2O_3, MeOH, H_2, 10 atm, 50 °C, 3.5 h, H-Cube®, then 10% Pd/C, MeOH, H_2, 60 atm, 60 °C, 6 h, H-Cube®, 50%; (d) 4M HCl in dioxane, CH_2Cl_2, rt, 4 h, quantitative; (e) xant-Phos (0.09 eq.), $Pd(OAc)_2$ (0.06 eq.), Ar-Br (1.3 eq.) Cs_2CO_3 (1.5 eq.), dioxane, 100 °C, 16 h, 19-38%; chiral chromatography (for **6**).

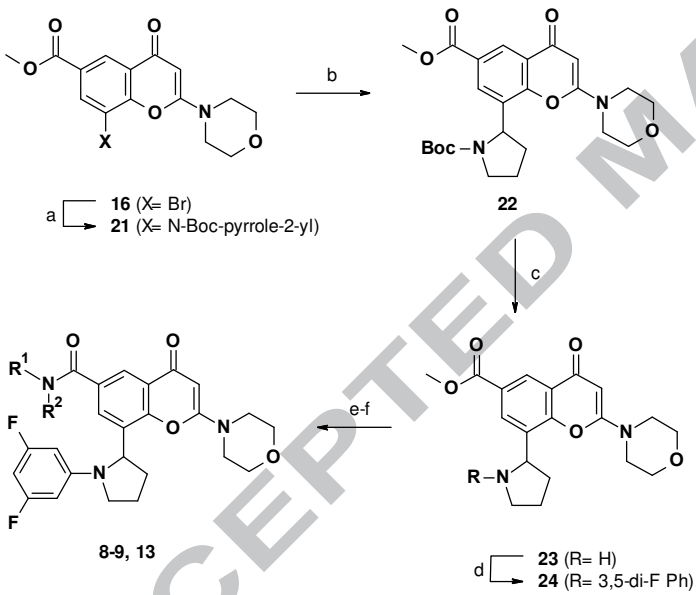

Scheme 2. Synthesis of compounds **8-9**, **13**. (a) *N*-Boc-pyrrole-2-boronic acid (1.1 eq), $(PPh_3)_2PdCl_2$ (0.02 eq.), Na_2CO_3, DME-water, 80 °C, 7 h, 70%; (b) 5% Rh/Al_2O_3, MeOH, H_2, 5 atm, 65 °C, 7 h, H-Cube®, 83%; (c) 4M HCl in dioxane, CH_2Cl_2, rt, 4 h, 83%; (d) Pd-catalyst (0.05 eq. ; made from: xant-Phos (2.2 eq.), Pd_2dba_3 (1 eq.), 1-bromo-3,5-difluorobenzene (9 eq.), benzene; precipitation in ether, 39%), Cs_2CO_3 (1.5 eq.), 1-bromo-3,5-difluorobenzene (1.1 eq.), dioxane, 80 °C, 23 h, 58%; (e) NaOH, MeOH, 40 °C, 23 h, 35%; (f) R^1R^2NH, TSTU or TBTU, NEt^iPr_2 or *N*-methylmorpholine, DMF or NMP, rt, 66-71%.

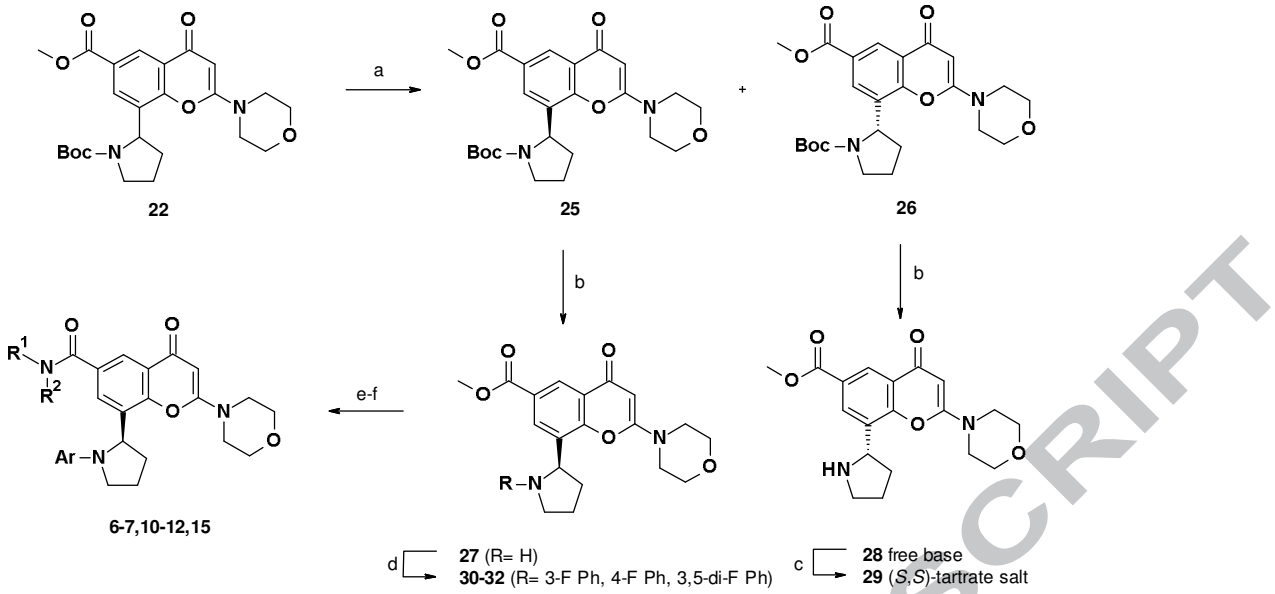

Scheme 3. Synthesis of compounds **6-7**, **10-12**, **15**. (a) chiral chromatography; (b) 4M HCl in dioxane, CH_2Cl_2, rt, 8 h, 88%; (c) (*S,S*)-tartaric acid, MeOH and isopropanol vapour diffusion crystallization; (d) $Pd(OAc)_2$ (0.05 eq.), xant-Phos (0.1 eq.), Cs_2CO_3 (1.5 eq.), aryl bromide (1.3 eq.), dioxane, 100 °C, 15 h; (e) NaOH, MeOH (f) R^1R^2NH, TSTU or TBTU or *n*Pr-phosphonic anhydride trimer, NEt^iPr_2, CH_2Cl_2 or $CHCl_3$, rt, 44-77%.

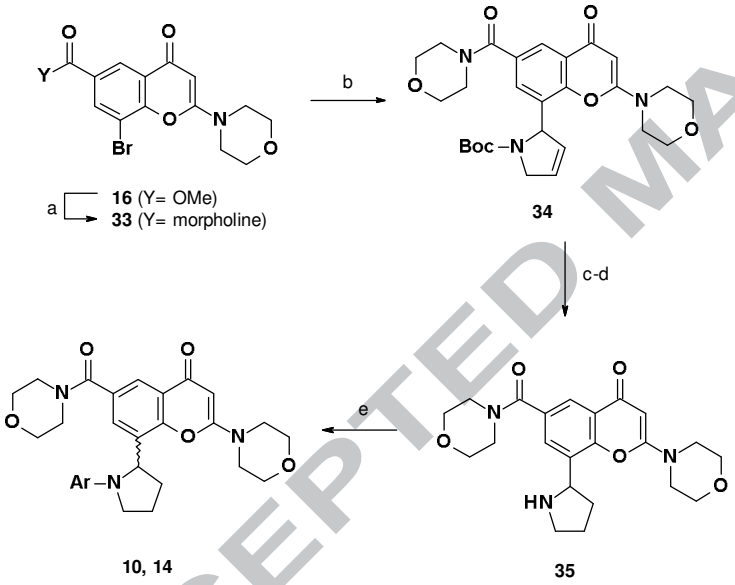

Scheme 4. Synthesis of compounds **10, 14**. (a) KOH (2 eq.), H_2O, rt, 4 h; morpholine (3 eq.), 2-Cl-4,6-MeO-1,3,5-triazine (4.3 eq.), *N*-methylmorpholine (0.5 eq.), H_2O, rt, 18 h, 78%; (b) *N*-Boc-2,3-dihydropyrrole (1.4 eq), PPh_3 (0.1 eq.), $Pd(OAc)_2$ (0.05 eq.), K_2CO_3, DMF, 100 °C, 16 h, 88%; (c) TFA, CH_2Cl_2, quantitative. (d) 5% Pd/C, MeOH, H_2, 5 atm, 45 °C, 3 h, H-Cube®, 53%; (e) xant-Phos (0.10 eq.), $Pd(OAc)_2$ (0.05 eq.), 1-bromo-3,5-difluorobenzene (1.3 eq.) Cs_2CO_3 (3 eq.), dioxane, 100 °C, 2 h, 75% (for **10**) or biphenyl-2-yldicyclohexylphosphine (0.10 eq.), $Pd(OAc)_2$ (0.05 eq.), 1-bromo-4-fluorobenzene (1.3 eq.), Cs_2CO_3 (1.5 eq.), dioxane, 100 °C, 15 h, 46% (for **14**); chiral chromatography.

Table 2. Biological activity of compounds **6, 10, 15** in different PI3K enzyme and cell assays**.**

cmpd	PI3Kα enz IC_{50}[a]	PI3Kβ enz IC_{50}[a]	PI3Kγ enz IC_{50}[a]	PI3Kδ enz IC_{50}[a]	PI3Kα cell IC_{50}[a]	PI3Kβ cell IC_{50}[a]	PI3Kγ cell IC_{50}[a]	PI3Kδ cell IC_{50}[a]
6	0.024	0.0067	0.33[b]	0.0082	0.18	0.0034	-	-
10	0.013	0.0071	0.19	0.0086	0.14	0.0011	1.5[b]	0.014
15	0.019	0.0061	0.34	0.0051	0.30	0.0028	-	-

[a] μM, numbers are a geometric mean of 2 or more values
[b] n=1

Table 3. Pharmacokinetic properties of compounds **10** and **15**.

Cpd	Mo/Dog CL[a]	Mo/Dog Vdss[a]	Mo/Dog F%[a]	Mo/Dog/Hu f_u[b]	Mo/Dog/Hu heps CL_{int}[c]
10	60 /23	1 / 1.2	26 / 29	19 / 28 / 17	68 / 23 / 2.7
15	47 / -	0.9 / -	18 / -	- / - / 11	134 / - / -

[a] Mouse and dog pharmacokinetic parameters from blood concentrations; hairy mice dosed at 5 µmol/kg i.v. and 30 µmol/kg p.o., dogs dosed at 4 µmol/kg i.v. and 10 µmol/kg p.o.; Clearance (mL/min/kg), Vdss (L/kg) and bioavailability (%).
[b] protein binding in mouse, dog or human plasma, expressed as fraction unbound (%).
[c] intrinsic clearance from mouse, dog or human hepatocytes, CL_{int} (mL/min/10^6 cell)

Acknowledgments

We would like to acknowledge the following scientists for their contribution to the synthesis, purification or characterization of the compounds: Christian Delvare, Delphine Dorison Duval, Nancy De Grace and Gordon Currie, and the members of the SAR Screening Groups for generating the cell and biochemical data. We would like to thank Anne Ertan (AstraZeneca Södertälje) for solving the structure of **29** by single crystal X-ray diffraction.

References and notes

1 a) Vanhaesebroeck, B.; Leevers, S. J.; Ahmadi, K.; Timms, J.; Katso, R.; Driscoll, P. C.; Woscholski, R.; Parker, P. J.; Waterfield, M. D. *Annu. Rev. Biochem.* **2001**, *70*, 535. b) Cantley, L. C. *Science* **2002**, *296*, 1655. c) Foster, F. M.; Traer, C. J.; Abraham, S. M.; Fry, M. J. *J. Cell Sci.* **2003**, *116*, 3037.

2 Fruman, D.A.; Rommel, C. *Nat. Rev. Drug Discovery* **2014**, *13*, 140.

3 a) Lannutti, B. J.; Meadows, S. A.; Herman, S. E. M.; Kashishian, A.; Steiner, B.; Johnson, A. J.; Byrd, J. C.; Tyner, J. W.; Loriaux, M. M.; Deininger, M.; Druker, B. J.; Puri, K. D.; Ulrich, R. G.; Giese, N. A. *Blood* **2011**, *117*, 591. b) Norman, P. *Expert Opin. Ther. Pat.* **2011**, 11, 1773

4 a) Wee, S.; Wiederschain, D.; Maira, S.-M.; Loo, A.; Miller, C.; de Beaumont, R.; Stegmeier, F.; Yao, Y.-M.; Lengauer, C. *Proc. Natl. Acad. Sci. U.S.A.* **2008**, *105*, 1357. b) Jia, S.; Liu, Z.; Zhang, S.; Liu, P.; Zhang, L.; Hyun, S.; Zhang, L. J.; Signoretti, S.; Loda, M.; Roberts, T. M.; Zhao, J. J. *Nature* **2008**, *45*, 776.

5 a) Certal, V.; Carry, J.C.; Halley, F.; Virone-Oddos, A.; Thompson, F.; Filoche-Romme, B.; Al-Ahmad, Y.; Karlsson, A.; Charrier, V.; Delorme, C.; Rak, A.; Abecassis, P.-Y.; Amara., C.; Vincent, L.; Bonnevaux, H.; Nicolas, J.-P.; Mathieu, M.; Bertrand, T.; Marquette, J.P.; Michot, N.; Benard, T.; Perrin, M.-A.; Lemaitre, O.; Guerif, S.; Perron, S.; Monget, S.; Gruss-Leleu, F.; Doerflinger, G.; Guizani, H.; Brollo, M.; Delvarre, L.; Bertin, L.; Richepin, P.; Loyau, V.; Garcia-Echeverria, C.; Lengauer, C.; Schio, L. *J. Med. Chem.*, **2014**, *57*, 903. b) Certal, V.; Halley, F.; Virone-Oddos, A.; Delorme, C.; Karlsson, A.; Rak, A.; Thompson, F.; Filoche-Rommé, B.; El-Ahmad, Y.; Carry, J.-C.; Abecassis, P.-Y.; Lejeune, P.; Vincent, L.; Bonnevaux, H; Nicolas, J.-P.; Bertrand, T.; Marquette, J.-P.; Michot, N.; Benard, T.; Below, P.; Vade, I.; Chatreaux, F.; Lebourg, G.; Pilorge, F.; Angouillant-Boniface, O.; Louboutin, A.; Lengauer, C.; Schio, L. *J. Med. Chem.*, **2012**, *55*, 4788. c) Yu, H; Michael L. Moore, M. L.; Erhard, K.; Hardwicke, M. A.; Lin, H.; Luengo, J. I.; McSurdy-Freed, J.; Plant, R.; Qu, J.; Raha, K.; Rominger, C. M.; Schaber, M. D.; Michael D. Spengler, M. D.; Rivero, R. A. *ACS Med. Chem. Lett.*, **2013**, *4*, 230.

6 Nylander, S.; Kull, B.; Björkman, J.A.; Ulvinge, J.C.; Oakes, N.; Emanuelsson, B.M.; Andersson, M.; Skäby, T., Inghardt, T., Fjellström, O; Gustafsson, D. *J. Thromb. Haemost.* **2012**, *10*, 2127.

7 a) Giordanetto, F.; Barlaam, B.; Berglund, S.; Edman, K.; Karlsson, O.; Lindberg, J.A.; Nylander, S.; Inghardt, T. *Bioorg. Med. Chem. Lett.* **2014**, *24*, 3936 b) Barlaam, B.; Cosulich, S.; Degorce, S.; Fitzek, M.; Giordanetto, F.; Green, S.; Inghardt, T.; Hennequin, L.; Hancox, U.; Lambert-van der Brempt, C.; Morgentin, R.; Pass, S.; Plé, P.; Saleh, T.; Ward, L. *Bioorg. Med. Chem. Lett.* **2014**, *24*, 3928.

8 Barlaam, B.; Cosulich, S.; Degorce, S.; Fitzek, M.; Green, S.; Hancox, U.; Lambert-van der Brempt, C.; Lohmann, J.-J.; Maudet, M.; Morgentin, R.; Pasquet, M.-J.; Péru, A.; Plé, P.; Saleh, T.; Vautier, M.; Walker, M.; Ward, L.; Warin, N. *J. Med. Chem.*, **2015**, *58*, 943.

9 Barlaam, B.; Cosulich, S.; Degorce, S.; Fitzek, M.; Green, S.; Hancox, U.; Lambert-van der Brempt, C.; Lohmann, J.-J.; Maudet, M.; Morgentin, R.; Péru, A.; Plé, P.; Saleh, T.; Ward, L.; Warin, N. *Bioorg. Med. Chem. Lett.* **2016**, *26*, 2318.

10 Selected representative compounds were evaluated against the four PI3K isoforms (enzyme and/or cell assays, see Table 2). Biological protocols for PI3K enzymes are available in Ref 8. Protocols for PI3Kα, PI3Kβ, PI3Kδ cellular assays are available in Ref 8 and for PI3Kγ cellular assay in Ref 14): PI3Kα, inhibition of AKT phosphorylation at Thr308 in PIK3CA mutant human breast ductal carcinoma BT474 cells; PI3Kβ, inhibition of AKT phosphorylation at Ser473 in PTEN null breast adenocarcinoma MDA-MB-468 cells; PI3Kδ, inhibition of AKT phosphorylation at Ser473 in Jeko-1 B cells; PI3Kγ, inhibition of AKT phosphorylation at Ser473 in mouse monocytic RAW264 cells.
When the enantiomers were separated, activity resided mainly in one enantiomer, with the other enantiomer being significantly less active (data not reported), as previously described for **TGX-221**, **AZD6482** and **1-4**.
It is worth noting that we assessed PI3K selectivity based on cellular rather than enzyme assays, some of the PI3K enzyme assays reached "tight binding conditions" for the most potent inhibitors. Copeland, R. A. Enzymes; 2nd Ed.; Wiley-VCH: New York, 2000; pp 305−317. Tight binding conditions: the concentration of functional enzyme for each PI3K isoform was determined as described in Ref. 8. The tight binding limit is half the concentration of functional enzyme which gave a tight binding limit of 10 nM for α/β and 15 nM for δ IC50 enzyme assays. The tight binding limit for γ was not reached and so could not be experimentally determined.

11 Barker, G.; McGrath, J.L.; Klapars, A.; Stead, D.; Zhou, G.; Campos, K. R.; O'Brien, P. J. Org. Chem. **2011**, *76*, 5936 and associated references.

12 The best conditions for this reaction involved deprotonation of *N*-Boc pyrrolidine, transmetallation with $ZnCl_2$ and Negishi coupling with **17**: 10 mol% $Pd(OAc)_2$, 12.5 mol% $P^tBu_3.HBF_4$ with the organozinc species (3 eq., made from deprotonation with (−)-sparteine / sec-butyllithium and transmetallation with $ZnCl_2$ in dry methyl t-butyl ether at −70 °C) at room temperature gave the expected pyrrolidine **19** in 25% yield, the enantiomeric excess was not assessed. The major side product of the reaction was the des-bromo compound from reduction of **17**.

13 The crystal structure of **29** has been determined by single-crystal X-ray diffraction technique at 200K. **29** was crystallised from MeOH - isopropanol. The absolute configuration around the chiral atom was determined as *S* by relating to the known stereo centre of the counter ion, (*S,S*)-tartaric acid. As a consequence, the configuration of compounds **6**,**7**,**10-12**,**15** was determined to be *R*. All experimental details and procedures are available in: Barlaam, B.C.; Degorce, S. L.; Lambert-Van der Brempt, C. M. P.; Lohmann, J.-J. M.; Ple, P. Preparation of phenylpyrrolidinylmorpholinooxochromenecarboxamide derivatives for use as PI3-kinase inhibitors *PCT Int. Appl.* (2012), WO 2012140419.
Characterization of compound **10**: ^{1}H NMR ($CDCl_3$) 1.96-2.17 (m, 3H), 2.45-2.57 (m, 1H), 3.07-3.83 (m, 14H), 3.83-3.95 (m, 4H), 5.07 (d, 1H), 5.58 (s, 1H), 5.92 (dd, 2H), 6.11 (ddt, 1H), 7.24 (d, 1H), 8.15 (s, 1H); MS-ESI *m/z* 526 $[MH]^+$; $[\alpha]^D_{20°}$: - 4.5° (14.8 mg in 2 mL of acetonitrile); Analytical HPLC, flow: 1 mL/min, Chiralpak ID, 4.6mm x 250mm, 5µm, eluent: EtOH/MeOH 50:50), t_R 17.73 min (other enantiomer t_R 13.52 min).

14 Barlaam, B. Cosulich, S.; Delouvrie, B.; Ellston, R.; Fitzek, M.; Germain, H.; Green, S.; Hancox, U.; Harris, C. S.; Hudson, K.; Lambert-van der Brempt, C.; Lebraud, H.; Magnien, F.; Lamorlette, M.; Le Griffon, A.; Morgentin, R.; Ouvry, G.; Page, K.; Pasquet, G.; Polanska, U.; Ruston, L.; Saleh, T.; Vautier, M.; Ward, L. *Bioorg. Med. Chem. Lett.* **2015**, *25*, 5155.

Table 1. Structure, PI3K cellular activity, human hepatocyte Cl_{int}, lipophilicity, solubility and permeability of compounds **5-15.**

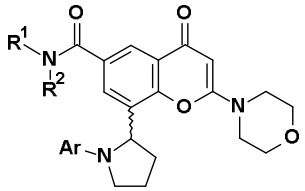

Cmpd	NR^1R^2	Ar	PI3Kβ cell IC_{50} (μM)[a]	PI3Kα cell IC_{50} (μM)[a]	Log $D_{7.4}$	Human hep. Cl_{int}[b]	Caco-2 P_{app}[d]	Mouse p.o. AUC[e]	Enantiomeric status[f]
5	NMe_2	Ph	0.0032	0.48	2.4	11	19	6.0	racemic
6	NMe_2	4-F Ph	0.0034	0.18	-	14	-	1.0	*R*
7	NMe_2	3-F Ph	0.0012	0.091	2.5	15	-	-	*R*
8	NMe_2	3,5-di-F Ph	0.0012	0.15	2.7	17	33	2.4	racemic
9	$N(Me)CH_2CH_2OH$	3,5-di-F Ph	0.0020	0.87	2.0	4	2.6	0.3	racemic
10	4-morpholine	3,5-di-F Ph	0.0011	0.14	2.5	2.7	18	2.8	*R*
11	4-Me-1-piperazine	3,5-di-F Ph	0.0023	0.25	2.3	11	3.3	-	*R*
12	azetidine	3,5-di-F Ph	0.0014	0.058[g]	2.9	9	-	-	*R*
13	4-OH-1-piperidine	3,5-di-F Ph	0.0030	0.63	2.3	<3	-	-	racemic
14	4-morpholine	4-F Ph	0.0045	1.2	2.2	8	-	-	note h
15	4-morpholine	3-F Ph	0.0028	0.30	2.2	6	14	1.7	*R*

[a] numbers are a geometric mean of 2 or more values.
[b] human hepatocyte intrinsic clearance, μL/min/10^6 cells.
[c] solubility from solid material, phosphate buffer (pH 7.4).
[d] apparent permeability from A (pH 6.5) to B (pH 7.4) in Caco-2 cell line, 10^{-6} cm/s.
[e] AUC after oral dosing (30 μmol/kg): hairy mice
[f] for compounds isolated as a pure enantiomer, absolute configuration.
[g] n=1
[h] Single enantiomer; absolute configuration not determined.

Graphical Abstract

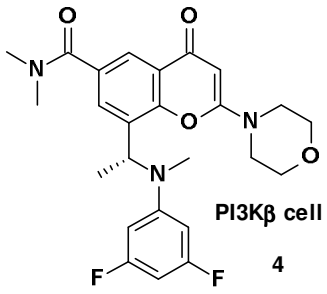

PI3Kβ cell IC_{50} 0.015 μM

4

Cyclisation
Conformational lock

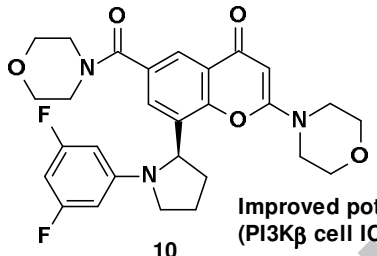

10

Improved potency
(PI3Kβ cell IC_{50} 0.0011 μM)
Excellent in vivo efficacy
(oral administration)